



THE UNIVERSITY *of* EDINBURGH

Edinburgh Research Explorer

## Model Predictive Control for Motion Planning of Quadrupedal Locomotion

### Citation for published version:

Shi, Y, Wang, P, Li, M, Wang, X, Jiang, Z & Li, Z 2019, Model Predictive Control for Motion Planning of Quadrupedal Locomotion. in *2019 IEEE 4th International Conference on Advanced Robotics and Mechatronics (ICARM)*. Institute of Electrical and Electronics Engineers (IEEE), pp. 87-92, IEEE International Conference on Advanced Robotics and Mechatronics (ICARM), Osaka, Japan, 3/07/19. <https://doi.org/10.1109/ICARM.2019.8834241>

### Digital Object Identifier (DOI):

[10.1109/ICARM.2019.8834241](https://doi.org/10.1109/ICARM.2019.8834241)

### Link:

[Link to publication record in Edinburgh Research Explorer](#)

### Document Version:

Peer reviewed version

### Published In:

2019 IEEE 4th International Conference on Advanced Robotics and Mechatronics (ICARM)

### General rights

Copyright for the publications made accessible via the Edinburgh Research Explorer is retained by the author(s) and / or other copyright owners and it is a condition of accessing these publications that users recognise and abide by the legal requirements associated with these rights.

### Take down policy

The University of Edinburgh has made every reasonable effort to ensure that Edinburgh Research Explorer content complies with UK legislation. If you believe that the public display of this file breaches copyright please contact [openaccess@ed.ac.uk](mailto:openaccess@ed.ac.uk) providing details, and we will remove access to the work immediately and investigate your claim.



# Model Predictive Control for Motion Planning of Quadrupedal Locomotion

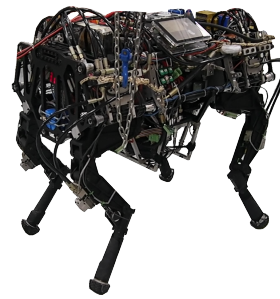
Yapeng Shi<sup>1</sup>, Pengfei Wang<sup>1</sup>, Mantian Li<sup>1</sup>, Xin Wang<sup>2</sup>, Zhenyu Jiang<sup>2</sup> and Zhibin Li<sup>3</sup>

**Abstract**—This paper is motivated to transfer the model predictive control approach used in bipedal locomotion to formulate gait planning of quadrupedal robots. The particular lateral-sequence gait of quadrupeds is treated as an equivalence to the bipedal walking. The Model Predictive Control (MPC) algorithm uses 3D-Linear Inverted Pendulum Model for representing the center of mass dynamics for planning the quadrupedal gaits, and a dimensionless discrete-time state-space formulated is derived for MPC. Subsequently, the footholds can be generated automatically via optimization of quadratic programming (QP) without the need of a separate footstep planner. The generated walking gaits were implemented and validated first in the physics simulation of a quadruped named EHbot, and then the effectiveness of the proposed method was further demonstrated through our experiments. Both simulation and experimental data are presented and analyzed for evaluating the performance.

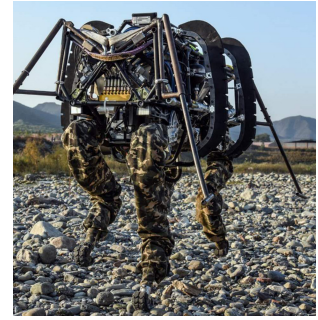
## I. INTRODUCTION

The advantage of wheels comes together with the invention of pavement and roads, and while facing difficult terrains, a biological setup such as legs has greater advantages in dealing with rugged surfaces, slopes, rocks, stairs, ledges, sand, and snow. Quadrupedal robots are one type of legged machines that are built for multi-terrain purposes [1], [2], [3], [4]. Quadrupedal robots exhibit various gait patterns, depending on the locomotion speed, terrain conditions as well as animal species [5], [6]. Furthermore, in low-speed locomotion, most mammalian use a so-called lateral-sequence walk (L-S walk) while walking, such as horse, lion and so on [7], [8]. L-S walk is one of the major gaits, where hind-limb foot placement is followed by the ipsilateral (same-side) forelimb [9].

In a complex environment, quadrupedal robots usually imitate the L-S walk gait of the mammalian to traverse at low speed. For better stability, the walking pattern generator drives the center of mass (CoM) to shift left and right periodically. So the behavior of quadrupedal locomotion is similar to that of bipeds. It is well known that the fundamental characteristics for the CoM of robots exhibit similar pattern and behavior of inverted pendulum-like dynamics during walking. Therefore, a lot of work has simplified the complex



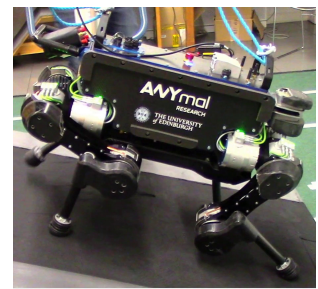
(a) Electro-hydraulic *EHbot*



(b) Hydraulic quadruped *Runner*



(c) Electric quadruped *Jueying*



(d) Electric quadruped *Anymal*

Fig. 1: Quadrupedal robots developed for rough-terrain mobility: (a) *EHbot* [1], (b) *Runner* [2], (c) *Jueying* [3], (d) *Anymal* [4].

dynamics of legged robots as an inverted pendulum model during walking [5], [10], [11], [12]. It is a simple yet effective way to avoid the model complexity and computational cost of the legged dynamics. Besides, it is easy to understand how the limbs produce inverted pendulum-like dynamics for bipeds.

Walking quadrupeds, however, are more difficult to be modeled as an inverted pendulum because of differences in the number of limbs. Raibert introduced the conception of “virtual leg” making complex gaits possible on four-legged robots such as trot, pace and bound, where there is only one equivalent “virtual leg” at a time during foot-ground contact. So that one-foot algorithm can be applied to control quadrupedal locomotion [13]. In some articles, quadrupedal gait is also equivalent to that of bipeds [14]. Following the idea of bipedal motion planning, the algorithm for generating a walking pattern for bipedal robots is a simple and effective way for the gait planning of quadruped robots.

So in this study, we are going to apply the method of bipedal gait generation for quadrupedal planning. In bipedal locomotion, a promising approach to generate walking mo-

<sup>1</sup>Yapeng Shi, Pengfei Wang and Mantian Li are with State Key Laboratory of Robotics and System, Harbin Institute of Technology, Harbin, 150001, China. shiyapeng66@163.com, wangpengfei1007@163.com, 15b908016@hit.edu.cn

<sup>2</sup>Xin Wang and Zhenyu Jiang are with Shenzhen academy of aerospace technology, China Aerospace Science, Shenzhen, 518057, China. xin.wang@chinasaat.com, for0207@126.com

<sup>3</sup>Zhibin Li is with School of Informatics, University of Edinburgh, UK. zhibin.li@ed.ac.uk

Corresponding authors are Mantian Li and Xin Wang.

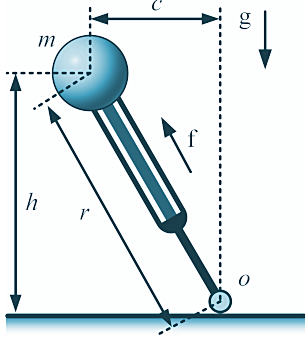


Fig. 2: The 3D linear inverted pendulum model with mass  $m$  and a massless leg: the point foot  $O$  is in contact with the ground, the height of the CoM remains constant at  $h$ , and the gravitational acceleration is  $g$ .

tions online is to use model predictive control (MPC) method for autonomous walking [15], [16], [17], [18], [19], [20]. Considering the task commands and the system constraints, MPC-based scheme can generate optimal trajectories within the predictive horizon, according to the current state of the system [21]. Inspired by these approaches [22], [23], this paper converts the quadrupedal L-S walk equivalently to bipedal motion. In addition, the model predictive control algorithm is derived for generating the quadruped L-S walk with automatic foothold optimization. The algorithm is then applied to generate the quadrupedal locomotion.

The remainder of this paper is organized as follows. In Sec. II, we present a dimensionless dynamics model for a quadruped system, based on which, the discrete state equation is obtained. Sec. III elaborates the details that convert the quadruped L-S walk equally to the bipedal motion. Following that, the model predictive control algorithm is derived in Sec. IV. After the implementation of the proposed method, Sec. V provides results of a series of simulations and experiments carried out on a quadruped robot - EHbot. Finally, the conclusion and future work are given in Sec. VI.

## II. DIMENSIONLESS DYNAMICS MODEL FOR QUADRUPED ROBOTS

Legged locomotion can be difficult to analyze and control due to the high dimensionality and nonlinearity of a legged system. Simple models are often used to study the balance strategy, and the most notable model of these is the 3D-Linear Inverted Pendulum Model (LIPM) [24], [25], [26], [27], which is linear due to the assumption that the height of the center of mass (CoM) is constant, and there are zero vertical acceleration and zero angular momentum. So in this study, we use LIPM as the prediction model for MPC.

The dynamics of the 3D-LIPM can be written as:

$$m\ddot{\bar{c}}^{x,y} = \frac{mg}{h}(\bar{c}^{x,y} - \bar{z}^{x,y}), \quad (1)$$

where  $m$  is the mass,  $\bar{c}^{x,y}$  is the  $xy$ -plane projective position of the center of mass (CoM),  $g$  is the gravitational acceleration vector,  $h$  is constant with the motion of the CoM kept on

a horizontal plane,  $\bar{z}^{x,y}$  denotes the location of the center of pressure (CoP) on the ground.

For the simplicity, equation of motion (1) can now be rewritten as:

$$\bar{z}^{x,y} = \bar{c}^{x,y} - T_0^2 \ddot{\bar{c}}^{x,y}, \quad (2)$$

where  $T_0 = \sqrt{h/g}$  is the time constant for the 3D-LIPM.

In order to reduce the number of related variables and simplify the subsequent derivations, the parameters intrinsic to the LIPM can be reduced to a dimensionless version of dynamics. The dimensional analysis is performed as follows, and the equations of motion can be normalized as:

$$z^{x,y} = c^{x,y} - \ddot{c}^{x,y}. \quad (3)$$

The dimensionless variables are as follows

$$t = \frac{\bar{t}}{T_0}, \quad z^{x,y} = \frac{\bar{z}^{x,y}}{h} \\ c^{x,y} = \frac{\bar{c}^{x,y}}{h}, \quad \dot{c}^{x,y} = \frac{\dot{\bar{c}}^{x,y}}{T_0 h}, \quad \ddot{c}^{x,y} = \frac{\ddot{\bar{c}}^{x,y}}{T_0^2 h} \quad (4)$$

We can see that the dimensional dynamics equation eliminate the height  $h$  and the time constant  $T_0$ . Note that this equation of motion is linear. This linearity is what makes the model computationally efficient and the direction of  $x, y$  decoupled, as it allows us to make closed form predictions. At the  $k^{th}$  sampling instant, with trajectories of the CoM which have a piecewise constant jerk over constant time intervals  $T$ . That way, the discrete-time state-space model can be described as:

$$\hat{c}_{k+1}^{x,y} = \bar{A}\hat{c}_k^{x,y} + \bar{B}\ddot{c}_k^{x,y}, \quad (5)$$

$$z_k^{x,y} = \bar{C}\hat{c}_k^{x,y}, \quad (6)$$

with

$$\hat{c}_k^{x,y} = [c_k^{x,y} \quad \dot{c}_k^{x,y} \quad \ddot{c}_k^{x,y}], \quad (7)$$

$$\bar{A} = \begin{bmatrix} 1 & T & \frac{T^2}{2} \\ 0 & 1 & T \\ 0 & 0 & 1 \end{bmatrix}, \quad \bar{B} = \begin{bmatrix} \frac{T^3}{6} \\ \frac{T^2}{2} \\ T \end{bmatrix}, \quad \bar{C} = \begin{bmatrix} 1 \\ 0 \\ -1 \end{bmatrix}, \quad (8)$$

where the decision variables are the state variable and control variable vectors respectively at the  $k_{th}$  sampling instant. Using the dimensionless dynamics equation (5) and (6) recursively, we can derive relationships between the position, velocity, acceleration and the jerk of the CoM, and the position of the CoP during the time intervals  $NT$ :

$$c_{k+1}^{x,y} = \begin{bmatrix} A \\ A^2 \\ \vdots \\ A^N \end{bmatrix} c_k^{x,y} + \begin{bmatrix} B & 0 & \cdots & 0 \\ AB & B \cdots & & 0 \\ \vdots & \vdots & \ddots & \vdots \\ A^{N-1}B & A^{N-2}B \cdots & & B \end{bmatrix} \ddot{c}_k^{x,y}, \quad (9)$$

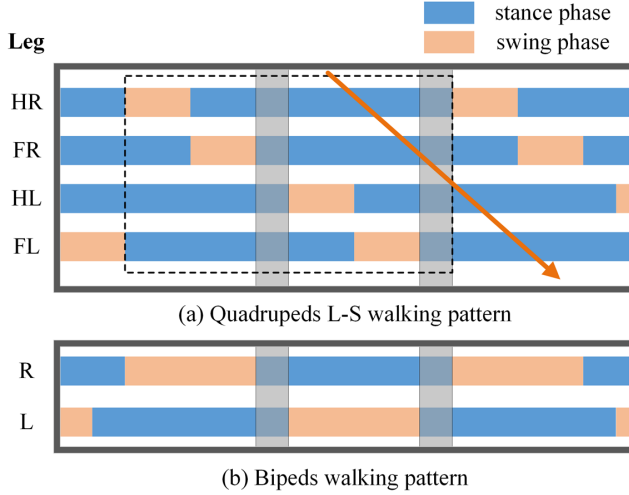


Fig. 3: Walking pattern of quadrupeds and bipeds. The simulations and experiments are implemented in this paper. The anterior-posterior sequence (APS) pattern is indicated by the arrow, which shows the logic inter-limb coordination. Beginning with the right hind limb lift, the stride cycle is bounded by the dashed rectangular outline. The gray shaded areas indicate the four-foot support phases for quadrupeds (double support phase for bipeds).

$$Z_k^{x,y} = \begin{bmatrix} CA \\ CA^2 \\ \vdots \\ CA^{N-1} \end{bmatrix} c_k^{x,y} + \begin{bmatrix} 0 & 0 & \cdots & 0 \\ CB & B \cdots & & 0 \\ \vdots & \vdots & \ddots & \vdots \\ CA^{N-2}B & CA^{N-3}B \cdots & & 0 \end{bmatrix} \ddot{C}_k^{x,y}, \quad (10)$$

with

$$C_{k+1}^{x,y} = [\hat{c}_{k+1}^{x,y}, \hat{c}_{k+2}^{x,y}, \dots, \hat{c}_{k+N}^{x,y}]^T, \quad (11)$$

$$\ddot{C}_k^{x,y} = [\ddot{c}_k^{x,y}, \ddot{c}_{k+1}^{x,y}, \dots, \ddot{c}_{k+N-1}^{x,y}]^T, \quad (12)$$

$$Z_k^{x,y} = [z_k^{x,y}, z_{k+1}^{x,y}, \dots, z_{k+N-1}^{x,y}]^T. \quad (13)$$

### III. WALKING PATTERN CONVERSION

For quadrupedal locomotion in the L-S walk mode, the behavior of a quadruped robot is similar to that of a biped system. So in this paper, we utilize the walking pattern generation of a biped robot for planning the quadrupedal locomotion.

In this study, the simulations and experiments are implemented by means of a particular walking pattern with a specific order and cycle. The overview of the gait cycle is shown in Fig. 3. The gait cycle follows the pattern: right hind (HR) to the right front (FR) to the left hind (HL) to left front (FL) leg. The anterior-posterior sequence (APS) pattern is indicated by the arrow, which shows the logic inter-limb coordination. The stride cycle is bounded by the dashed

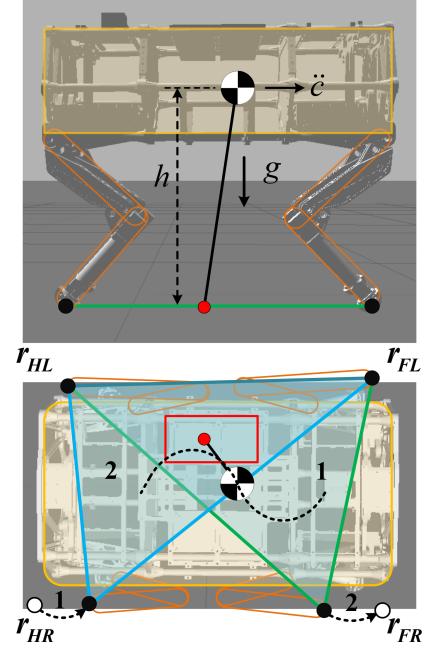


Fig. 4: Walking pattern conversion from quadrupeds to bipeds during L-S walk. The support triangles 1, 2 are supporting polygons during walking. The red rectangle is a conservative support polygon through simple linearization.

rectangular outline. The gray shaded areas indicate the four-foot support phases for quadrupeds (double support phases for bipeds).

For the quadrupedal L-S walk, only one foot is lifted from the ground at a time, while the other three feet maintain a stable tripodal stance. In other words, the torso of the quadruped robot is supported by at least three points in contact with the ground at all times, which form a supporting polygon. Besides, the torso shifts periodically left and right during walking. The CoM is shifted over the current support triangle before the swing motion of a leg is initiated. As shown in Fig. 3, before the HR leg is to be lifted and placed forward, the CoM of the robot is shifting to the left to gain better stability. While the HR leg is in the swing phase, the other three support feet constitute a support triangle. The CoP of the LIPM has to lie within the support triangle 1. Followed by the HR leg touching the ground, the same-side forelimb, the FR leg is then lifted and placed forward and the CoP lies within the support triangle 2.

As can be seen from Fig 2, if we assume the HR and FR legs of quadrupeds as the right virtual leg of bipeds. Similarly, the HL and FL legs of the quadruped are regarded as the left virtual leg of humanoid robots. Thereby, the quadrupeds walking pattern (Fig. 3a) can be converted to the bipedal walking patterns (Fig. 3b). Therefore, the constrained region of the CoP is the intersection area of these triangular support polygons.

As we can see from the figure, the constrained regions are nonlinear. Since formulating the MPC problem in the quadratic programming (QP) form requires linear constraints,

in order to allow fast computation for real-time execution, as well as for faster control loops, the constraints hence must be linearized. As shown in Fig. 3, the conservative constraint region is bounded by the red rectangular approximation through a simple linearization, where the red rectangle is the constraint of the CoP for optimization. Note that the size of the rectangular support can be set by taking into account the compromise between flexibility and safety margin.

#### IV. MODEL PREDICTIVE CONTROL APPROACH

For bipedal locomotion, the traditional approaches usually give a set of footholds by a footstep planner. The trajectory of the CoM is generated by both GRFs and contact positions. So the torso acceleration and the footholds are mutually determined. Therefore, the drawback of these methods is that the predefined footholds strongly restrict the feasibility and robustness of the locomotion. Compared with pre-planned footholds according to the footstep planner, an approach of adaptive footholds is a more effective way to deal with the problem [23]. Inspired by this, the reference position of the CoP are actually generated as:

$$Z_{k+1}^{ref} = VP_k^{x,y} + \tilde{V}\tilde{P}_k^{x,y} \quad (14)$$

with

$$V = \begin{pmatrix} 1 \\ \vdots \\ 1 \\ 0 \\ \vdots \\ \vdots \\ 0 \\ 0 \\ \vdots \\ 0 \end{pmatrix}, \quad \tilde{V} = \begin{pmatrix} 0 & 0 \\ \vdots & \vdots \\ 0 & 0 \\ 1 & 0 \\ \vdots & \vdots \\ 1 & 0 \\ 0 & 1 \\ \vdots & \vdots \\ 0 & 1 & \ddots \end{pmatrix} \quad (15)$$

Among the first elements of the vector  $V \in \mathbb{R}^N$ , the number 1 indicates the current step, which means the support legs are unchanged. And the number 1 in the matrix  $\tilde{V} \in \mathbb{R}^{N \times m}$  indicates the future support legs sampled within the next several steps. In this paper, we set the number of total steps  $m$  in a moving horizon window of three steps.

For the quadrupedal locomotion, the robot has to track the planned motion while keeping balance. So the cost function used in the MPC is defined by

$$J = \frac{w_0}{2} \left\| C_{k+1}^{x,y} - C_{k+1}^{ref} \right\|_2^2 + \frac{w_1}{2} \left\| \dot{C}_{k+1}^{x,y} - \dot{C}_{k+1}^{ref} \right\|_2^2 + \frac{w_2}{2} \left\| Z_{k+1}^{x,y} - Z_{k+1}^{ref} \right\|_2^2 + \frac{w_3}{2} \left\| \ddot{C}_k^{x,y} \right\|_2^2, \quad (16)$$

where  $w_0$ ,  $w_1$ ,  $w_2$  and  $w_3$  are weights, the first term is for tracking the reference trajectory of the CoM. We set the CoM reference between the current foothold and the next foothold, so as to guarantee the locomotion stability and robustness. The second and third terms serve to follow the reference velocity of the CoM and to track the reference ZMP for the feasibility of ground reaction forces. The fourth term is also

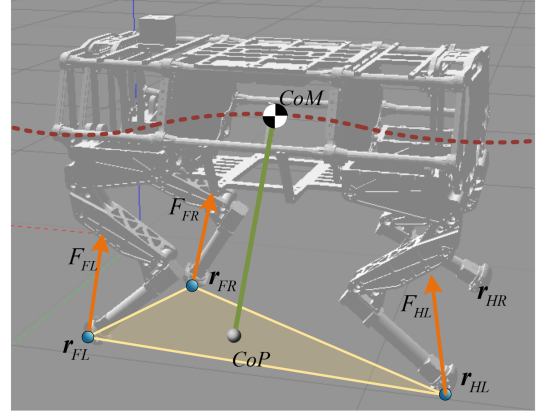


Fig. 5: Simulated EHbot in Gazebo for quadruped L-S walk.

desirable for minimizing the CoM jerk to produce smooth trajectories.

There are four weighted combinations of the cost function. This MPC optimization problem can be reformulated as a quadratic programming (QP) as:

$$J = \frac{1}{2} U_k^T Q_k U_k + f_k^T U_k \rightarrow \min. \quad (17)$$

The control variables are:

$$U_k = [\ddot{C}_k^x, \tilde{P}_k^x, \ddot{C}_k^y, \tilde{P}_k^y]^T. \quad (18)$$

It is important to note that the control variables include the jerk of the CoM and the next foothold that needs to be optimized. The linear MPC optimization problem can be solved by most programming solves, such as FMINCON, IPOPT [28] and qpOASES [29].

Once we obtain the optimal CoM trajectories and the bipedal footholds, then the quadruped feet trajectories can be generated with fixed offsets according to the size of the quadruped robot. Furthermore, we use a cubic polynomial for plan a continuous swing foot trajectories for reducing the ground impact of the instant change of velocity during the swing leg touch-down, which is a third-degree polynomial equation that can generate a trajectory from its initial and the desired final point optimized as follows:

$$\begin{aligned} x &= a_0 + a_1 t + a_2 t^2 + a_3 t^3, \\ \dot{x} &= a_1 + 2a_2 t + 3a_3 t^2, \\ \ddot{x} &= 2a_2 + 6a_3 t, \end{aligned} \quad (19)$$

where  $a_0$ ,  $a_1$ ,  $a_2$ , and  $a_3$  being the function parameters. The acceleration profile of cubic polynomial is continuous and changes linearly over time. The values of coefficients are shown as follows:

$$\begin{aligned} x(t_0) &= r_0^f, \dot{x}(t_0) = \dot{r}_0^f, \\ x(t_d) &= r_d^f, \dot{x}(t_d) = \dot{r}_d^f, \end{aligned} \quad (20)$$

where  $r_0^f$  and  $r_d^f$  are the initial position and desired position in a definite amount of time  $[t_0, t_d]$ , separately. Under normal condition,  $\dot{r}_0^f$  and  $\dot{r}_d^f$  are both zero.

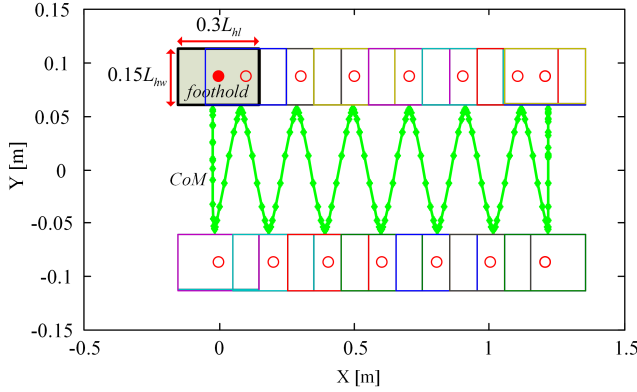


Fig. 6: The simulated results for the quadruped L-S walk. The foot size of the virtual biped is  $0.3L_{hl} \times 0.15L_{hw}$ .  $L_{hl} = 0.5m$  is half the distance of front-hind legs of the quadruped in normal stance. While  $L_{hw} = 0.175m$  is half the distance between the left and right legs of the quadruped. The red circular markers are the centers of virtual feet and green asterisk markers are the CoM trajectories.

## V. RESULTS

In the preview section, we obtained the optimal trajectories of the CoM and the feet by utilizing the MPC algorithm. In this section, the proposed trajectories are implemented both in simulations and experiments for validating the proposed method. The performance of the quadrupedal locomotion is evaluated on an electro-hydraulic quadruped prototype, EHbot. The detail information of the quadruped platform can be found in [1]. Video for the tests is available through the accompanying video of this paper.

Through the MPC planning based on the proposed method, we can obtain the optimal COM trajectory and the footholds. Then the controller must follow the required motion as well as considering the compliant interaction. So in this paper, we introduce a force control approaches to tracking the desired trajectory in the Cartesian space proposed in [30].

Our primary tests were conducted in the physics-based simulator first - ROS-Indigo and Gazebo 7.12.0 [31]. As shown in Fig. 4, we have built the quadruped model, EHbot, sensors and other parameters in Gazebo to simulate a realistic environment. As we can easily monitor the system parameters and apply them to a real quadruped robot with C++ code.

As shown in Fig. 3, the step duration is  $T_{step} = 2.0s$ . The duration of four legged supporting is  $T_{fsp} = 0.4s$  for all tasks. The sampling interval for discretization is  $\delta T = 0.05s$ . Meanwhile, we insert an initial stance phase of  $T_{ini} = 1.0s$  to allow sufficient time to initialize the body before taking the first step.

As shown in Fig. 6, the graph shows the virtual biped robot, move forward (quadruped robot, EHbot with L-S walk). The CoM trajectory of the quadruped system shifts left and right periodically just as the bipeds do during walking. The rectangle represents a virtual biped foot. The size of the feet is  $0.3L_{hl} \times 0.15L_{hw}$ .  $L_{hl} = 0.5m$  is half

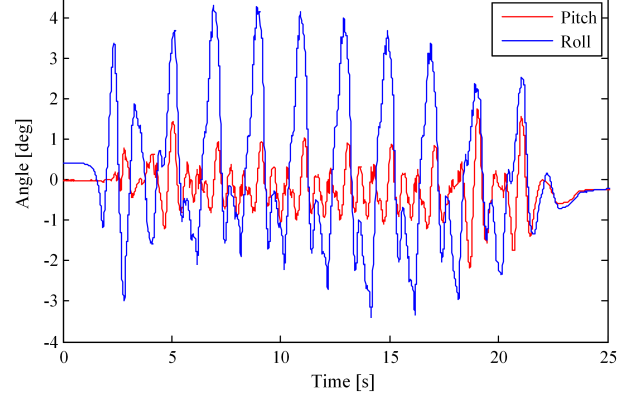


Fig. 7: The experimental results of the pitch (solid red line) and roll (solid blue line) angles of the body orientation during the quadruped L-S walk based on the MPC method. The amplitude of roll angle is stabilized within 4.5 degrees.

distance between quadruped front and hind legs under the normal standing situation. While  $L_{hw} = 0.175m$  represents half the distance between the left and right legs of the quadruped robot, EHbot. The geometric center of the virtual feet is marked as red circles. Green asterisk markers indicate the CoM trajectories of the quadruped robot.

In addition, the algorithm has been further validated on a real quadruped prototype, EHbot. It has been demonstrated that the quadruped robot performed the L-S walk with the proposed method (see Fig. 7 and Fig. 8). As shown in Fig. 7, the pitch and roll angles of the torso fluctuate within a narrow range, where maximum changes of amplitudes are less than 2.2 degrees and 4.5 degrees, respectively. Furthermore, we note that the roll angle amplitude is asymmetric due to the asymmetric distribution of the torso mass. Fig. 8 depicts the snapshots of these experiments. The results of the tests demonstrate that the proposed algorithm is effective for realizing the quadruped L-S walk.

## VI. CONCLUSION AND FUTURE WORK

In this article, we present a linear MPC algorithm for specifically generating quadruped lateral-sequence (L-S) walk. Based on LIPM, a dimensionless discrete-time state-space is derived for quadruped dynamics. Inspired by the bipedal locomotion, a walking pattern conversion was implemented from bipedal walking to the quadruped L-S walking. The linear approximation of the constraint region of the CoP was then formulated. Following that, we derived the MPC algorithm with both CoM trajectory and foothold that can be optimized as a QP problem. Finally, the proposed algorithm has been validated both in simulation and experiment which demonstrated the effectiveness of the proposed method.

However, there are some limitations to this algorithm. One is the trade-off between the flexibility and safety margin during walking pattern conversion. Therefore, the method can restrict the flexibility of quadrupedal locomotion which is undesirable to some degrees. In addition, because of the walking pattern conversion, the proposed method remains

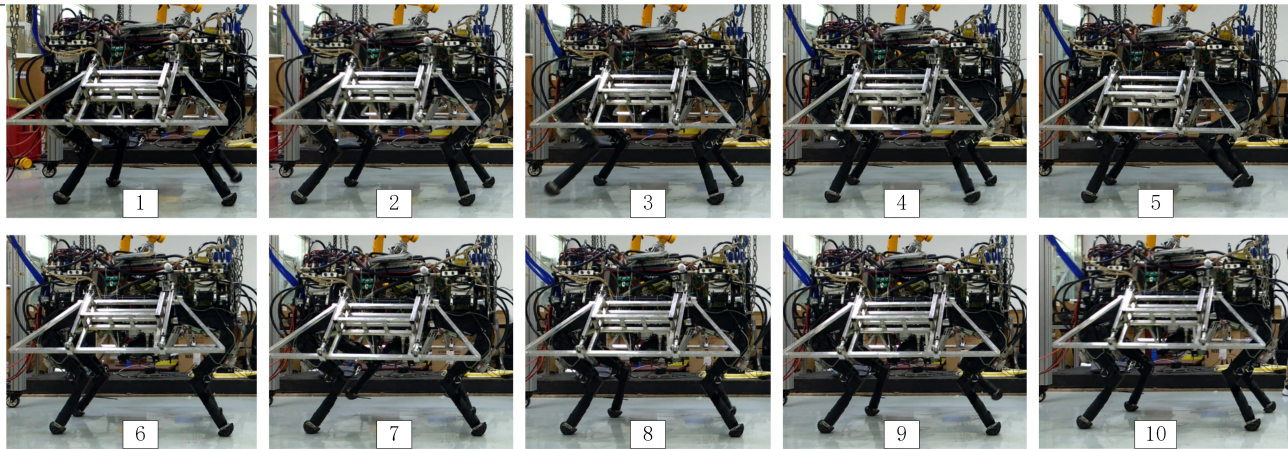


Fig. 8: The snapshots from the L-S walk experiment on the quadruped prototype, EHbot.

efficient specifically for quadruped L-S walk but not suitable to be generalized for high-speed quadrupedal gaits, like bound, pace, trot, or gallop. In future work, we would like to translate and adapt the idea of the proposed method for the motion planning of all types of gaits for quadruped robots.

#### REFERENCES

- [1] P. Wang, *et al.*, "An analytic solution for the force distribution based on cartesian compliance models," *International Journal of Advanced Robotic Systems*, vol. 16, no. 1, p. 172988141982747, 2019.
- [2] R. Dang, *et al.*, "The motion analysis and trajectory planning of static gait for the quadruped robot," in *20th international conference on climbing and walking robots and the support technologies for mobile machine (CLAWAR 2017)*, Proto, Portugal., 2017.
- [3] "Chinas Jueying Quadruped Robot," IEEE Spectrum. [Online]. Available: [spectrum.ieee.org/automaton/robotics/artificial-intelligence](http://spectrum.ieee.org/automaton/robotics/artificial-intelligence)
- [4] G. Xin, *et al.*, "A model-based hierarchical controller for legged systems subject to external disturbances," in *IEEE International Conference on Robotics and Automation*, 2018, pp. 4375–4382.
- [5] M. H. Raibert, *et al.*, "Bigdog, the rough-terrain quadruped robot," *IFAC Proceedings Volumes*, vol. 41, no. 2, pp. 10 822–10 825, 2008.
- [6] B. Boudon, *et al.*, "Bio-inspired topological skeleton for the analysis of quadruped kinematic gait," *Journal of Bionic Engineering*, vol. 15, no. 5, pp. 839–850, 2018.
- [7] G. B. Gillis, "Walk on four legs not on two," *The Journal of Experimental Biology*, vol. 207, no. 5, pp. 713–714, 2004.
- [8] M. Hildebrand, "Symmetrical gaits of horses," *Science*, vol. 150, no. 3697, pp. 701–708, 1965.
- [9] D. Owaki, *et al.*, "Simple robot suggests physical interlimb communication is essential for quadruped walking," *Journal of the Royal Society Interface*, vol. 10, no. 78, pp. 20 120 669–20 120 669, 2012.
- [10] S. Kajita, *et al.*, "Biped walking pattern generation by a simple three-dimensional inverted pendulum model," *Advanced Robotics*, vol. 17, no. 2, pp. 131–147, 2003.
- [11] Z. Li, *et al.*, "Walking trajectory generation for humanoid robots with compliant joints: Experimentation with coman humanoid," in *IEEE International Conference on Robotics and Automation*, 2012, pp. 836–841.
- [12] S. Caron and A. Kheddar, "Dynamic walking over rough terrains by nonlinear predictive control of the floating-base inverted pendulum," *intelligent robots and systems*, pp. 5017–5024, 2017.
- [13] M. H. Raibert, *et al.*, "Running on four legs as though they were one," *international Conference on Robotics and Automation*, vol. 2, no. 2, pp. 70–82, 1986.
- [14] J. Zhang, *et al.*, "Trot gait design and cpg method for a quadruped robot," *Journal of Bionic Engineering*, vol. 11, no. 1, pp. 18–25, 2014.
- [15] S. Faraji, *et al.*, "Versatile and robust 3d walking with a simulated humanoid robot (atlas): A model predictive control approach," in *IEEE International Conference on Robotics and Automation*, 2014, pp. 1943–1950.
- [16] J. A. Castano, *et al.*, "Enhancing the robustness of the epsac predictive control using a singular value decomposition approach," *Robotics and Autonomous Systems*, vol. 74, pp. 283–295, 2015.
- [17] S. Caron and A. Kheddar, "Multi-contact walking pattern generation based on model preview control of 3D COM accelerations," *IEEE-RAS international conference on humanoid robots*, pp. 550–557, 2016.
- [18] J. A. Castano, *et al.*, "Robust model predictive control for humanoids standing balancing," in *2016 International Conference on Advanced Robotics and Mechatronics (ICARM)*, 2016, pp. 147–152.
- [19] M. Naveau, *et al.*, "A reactive walking pattern generator based on nonlinear model predictive control," *IEEE Robotics and Automation Letters*, vol. 2, no. 1, pp. 10–17, 2017.
- [20] K. Yuan and Z. Li, "An improved formulation for model predictive control of legged robots for gait planning and feedback control," *IEEE/RSJ International Conference on Intelligent Robots and Systems*, pp. 8535–8542, 2018.
- [21] M. Neunert, *et al.*, "Whole-body nonlinear model predictive control through contacts for quadrupeds," *IEEE Robotics and Automation Letters*, vol. 3, no. 3, pp. 1458–1465, 2018.
- [22] S. Kajita, *et al.*, "Biped walking pattern generation by using preview control of zero-moment point," *International Conference on Robotics and Automation*, vol. 2, pp. 1620–1626, 2003.
- [23] A. Herdt, *et al.*, "Online walking motion generation with automatic footstep placement," *Advanced Robotics*, vol. 24, no. 5-6, pp. 719–737, 2010.
- [24] B. J. Stephens and C. G. Atkeson, "Push recovery by stepping for humanoid robots with force controlled joints," *IEEE-RAS International Conference on Humanoid Robots*, pp. 52–59, 2010.
- [25] M. Li, *et al.*, "Control of a quadruped robot with bionic springy legs in trotting gait," *Journal of Bionic Engineering*, vol. 11, no. 2, pp. 188–198, 2014.
- [26] J. A. Castano, *et al.*, "Dynamic and reactive walking for humanoid robots based on foot placement control," *International Journal of Humanoid Robotics*, vol. 13, no. 02, p. 1550041, 2016.
- [27] Q. Li, *et al.*, "Robust foot placement control for dynamic walking using online parameter estimation," *IEEE-RAS International Conference on Humanoid Robots*, pp. 165–170, 2017.
- [28] L. T. Biegler and V. M. Zavala, "Large-scale nonlinear programming using ipopt : An integrating framework for enterprise-wide dynamic optimization," *Computers & Chemical Engineering*, vol. 33, no. 3, pp. 575–582, 2009.
- [29] H. J. Ferreau, *et al.*, "qpocps: a parametric active-set algorithm for quadratic programming," *Mathematical Programming Computation*, vol. 6, no. 4, pp. 327–363, 2014.
- [30] Y. Shi, *et al.*, "Bio-inspired equilibrium point control scheme for quadrupedal locomotion," *IEEE Transactions on Cognitive and Developmental Systems*, pp. 1–1, 2018.
- [31] N. P. Koenig and A. Howard, "Design and use paradigms for gazebo, an open-source multi-robot simulator," *IEEE/RSJ International Conference on Intelligent Robots and Systems*, vol. 3, pp. 2149–2154, 2004.